Magnetic Porous Materials

DOI: 10.1002/anie.200604284

Dehydration-Induced Conversion from a Single-Chain Magnet into a Metamagnet in a Homometallic Nanoporous Metal–Organic Framework**

Xian-Ming Zhang, Zheng-Ming Hao, Wei-Xiong Zhang, and Xiao-Ming Chen*

The construction of homometallic porous metal–organic frameworks (MOFs) with interesting magnetic behavior is currently a challenging target because magnetism and porosity are mutually inimical.[1,2] Magnetic superexchange requires moment carriers that are separated through short bridges, while porosity generally relies on the use of long bridging ligands.[1–3] Despite this challenge, some notable successes have achieved in the area, such as the discovery of the solvatomagnetic effect.[4]

To design a porous homometallic MOF showing interesting magnetic behavior, we chose cobalt hydroxide chains containing triangular subunits as the rod-shaped secondary building units (SBUs) and benzotriazole-5-carboxylates as the bridging ligands. The intrinsic packing arrangement of rod-shaped SBUs may prevent interpenetration to guarantee a porous MOF.[5] The triangular magnetic lattice in combination with the large anisotropy of the Co^{II} ions can lead to unusual magnetic behaviors, such as multiple area of bistability.[6,7] Furthermore, desolvation and solvation in the synthesized MOF may induce various magnetic transitions.[4] The expectation is realized in the hydrated phase $[Co_3(OH)_2(btca)_2]\cdot 3.7H_2O$ (**1**·3.7 H_2O) and the dehydrated phase $[Co_3(OH)_2(btca)_2]$ (**1**; H_2btca = benzotriazole-5-carboxylic acid) which are 3D homometallic MOFs with the "sra" topology (analogous to that of the aluminum net in $SrAl_2$).[5] The dehydrated phase **1** shows field-induced metamagnetism whereas the hydrated phase **1**·3.7 H_2O is characteristic of ferrimagnetism and single-chain-magnet-like behavior.

[*] Prof. Dr. X.-M. Zhang, Z.-M. Hao
School of Chemistry and Material Science
Shanxi Normal University
Linfen 041004 (P.R. China)
Fax: (+86) 357-205-1402
E-mail: zhangxm@dns.sxnu.edu.cn
W.-X. Zhang, Prof. Dr. X.-M. Chen
MOE Key Laboratory of Bioinorganic and Synthetic Chemistry
School of Chemistry and Chemical Engineering
Sun Yat-Sen University
Guangzhou 510275 (P.R. China)

[**] This work was financially supported by the NSFC (20401011), the FANEDD (200422), the Program for New Century Excellent Talents in University (NCET-05-0270), the Youth Academic Leaders of Shanxi Program, and the Education Bureau of Shanxi. Special thanks to one of the referees who pointed out the single-chain-magnetic behavior of the hydrated phase.

Supporting information for this article is available on the WWW under http://www.angewandte.org or from the author.

The solvothermal treatment of a mixture of H_2btca, $Co(NO_3)_2\cdot 6H_2O$, CH_3CN, and H_2O in a molar ratio of 1:1.7:192:556 at 150 °C in a Teflon-lined stainless autoclave for 5 days resulted in red block crystals of the hydrated phase **1**·3.7 H_2O in 35 % yield. Elemental analysis, IR spectroscopy, thermal gravimetric analysis (TGA), and X-ray crystallography confirmed the formula of as-synthesized **1**·3.7 H_2O. The TGA trace of the as-synthesized **1**·3.7 H_2O in air shows that the trapped solvent water molecules can be easily removed at 95 °C and that the resulting dehydrated nanoporous MOF **1** is stable up to 310 °C (Supporting Information, Figure S1). A bulk sample of **1** was prepared by the calcination of **1**·3.7 H_2O at 105 °C for 8 h, and the structure was confirmed by single-crystal and powder X-ray diffraction (PXRD) analyses (Supporting Information, Figure S2). Some minor disagreements in the intensities of peaks in the simulated and measured PXRD patterns are due to preferred orientations of the microcrystals. The solvent water molecules in **1**·3.7 H_2O can also cause minor disagreements.

Compound **1**·3.7 H_2O is a 3D neutral MOF featuring 1D nanosized rhombic channels constructed from ferrimagnetic cobalt hydroxide chains and btca linkers. Each asymmetric unit consists of two crystallographically independent Co^{II} ions, one btca, and one μ_3-OH group as shown in Figure 1. The Co1 atom is coordinated by two OH groups, two nitrogen atoms, and two oxygen atoms from two btca ligands, in an octahedral geometry. The Co2 site has a distorted square-pyramidal coordination geometry and is ligated by two OH groups, two nitrogen atoms, and one btca oxygen atom. The Co^{II} ions are bridged by μ_3-OH groups to form a $Co_3(OH)_2$ chain (Figure 1 b)in which three adjacent Co^{II} ions are arranged into an approximate isosceles triangle. Each isosceles triangle is formed by two inversely related Co2 atoms (Co2 and Co2e) and one Co1 atom with Co···Co distances of 3.224(2), 3.286(2), and 3.560(2) Å. The Co1-O-Co2, Co1-O-Co2e, and Co2-O-Co2e angles are 109.0(1), 116.1(2), and 101.0(2)°, respectively. The $\{Co_3(OH)_2\}$ chains are linked by btca ligands in the μ_5 mode to furnish the 3D MOF with 1D nanosized rhombic channels running along the *c* axis (Figure 1 c). The topology of **1**·3.7 H_2O is an sra net.[5]

Single-crystal X-ray analysis of **1** shows that the 3D framework remains intact upon dehydration. Compared with **1**·3.7 H_2O, the average Co–L (L = N, O) length in dehydrated **1** is contracted by 0.003 Å. The changes in the Co-O-Co angles are limited to 0.3° (Co-O-Co angles, 108.9(3), 116.4(3), 101.1(3)° in **1**). After exclusion of the van der Waals radii of the surface atoms, the free area of the channels in **1** is approximately 12×7 Å^2. A calculation with PLATON[8]

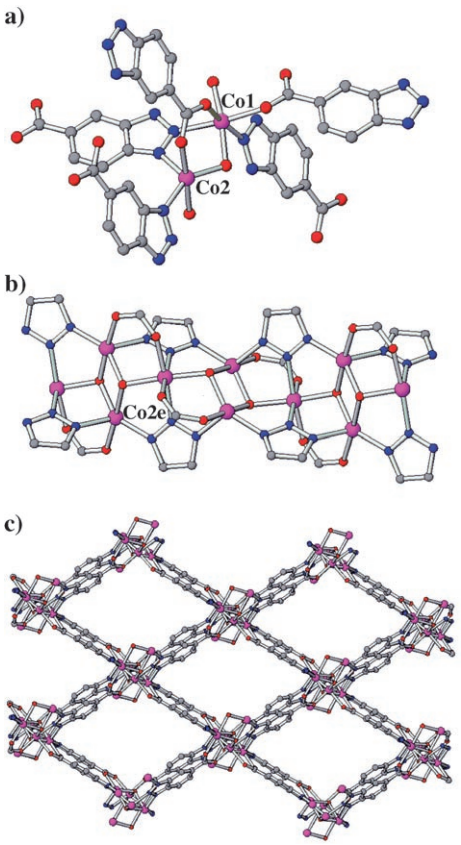

Figure 1. The coordination environments of the cobalt ions (a) and the Co–O chain (b; for clarity the btca ligands are truncated) in the 3D porous MOF **1**·3.7 H_2O (c); pink Co, red O, blue N, gray C; H atoms omitted for clarity.

reveals that the free volume of the channels is 948 Å^3 per unit cell, or 39.1 % of the total volume. The permanent porosity of **1** was confirmed by gas-sorption isotherm experiments performed in liquid nitrogen (Supporting Information, Figure S3). The calculated Langmuir surface area is 125 $m^2 g^{-1}$, while the micropore volume is 0.088 $cm^3 cm^{-3}$ (0.06 $cm^3 g^{-1}$).

The temperature dependence of the magnetic susceptibility for newly prepared **1**·3.7 H_2O in the temperature range 2–320 K under an applied field of 1 KOe was studied with a Quantum Design SQUID MPMS XL-7. The $\chi_m T$ value is 7.06 $cm^3 K mol^{-1}$ at 320 K, and it decreases with decreasing temperature down to a minimum value of 2.78 $cm^3 K mol^{-1}$ at 19 K (Supporting Information, Figure S4). Upon further cooling, the $\chi_m T$ value rapidly increases to a maximum of 10.21 at 5 K, and then decreases to 5.94 at 2 K. The average effective magnetic moment of 4.34 μ_B per cobalt atom at room temperature is higher than the expected spin-only value of 3.87 μ_B for a high-spin Co^{II} ion, but close to the moment of 4.40 μ_B observed in $[Co(N_2H_4)_2(acetate)_2]$.[9] A fitting to the Curie–Weiss law gives $C = 8.30$ $cm^3 K mol^{-1}$ and $\theta = -57.7$ K. Because of the lack of an analytical expression for an anisotropic model, an alternating 1D Heisenberg chain ($S = 3/2$) model ($H = -J_1\Sigma(S_{3i}S_{3i+1} + S_{3i+1}S_{3i+2}) - J_2\Sigma S_{3i-1}S_{3i}$, where J_1 is the intrachain coupling between Co1 and Co2 ions and J_2 is the intrachain coupling between Co2 ions) could be used, approximately.[10a] The best fitting gives $J_1 = -20.2(4)$ cm^{-1}, $J_2 = 2.1(3)$ cm^{-1}, $g = 2.40(1)$, and $R = 1.42 \times 10^{-5}$, $R = [(\chi_m T)_{obsd} - (\chi_m T)_{calcd}]^2/[(\chi_m T)_{obsd}]^2$ (Supporting Information, Figure S5). In addition, we attempted to fit the magnetic data by using the above alternating 1D Heisenberg chain ($S = 3/2$) model with an orbital correction term θ. The fitting resulted in a set of less reasonable parameters: $J_1 = -19.7(3)$ cm^{-1}, $J_2 = -5.0(3)$ cm^{-1}, $g = 2.40(1)$, $\theta = 8.3(2)$ K, and $R = 3.6 \times 10^{-5}$ (Supporting Information, Figure S6). For a perfect octahedral Co^{II} complex, the estimated orbital contribution is approximately −20 K, and the distortion of octahedron can decrease the orbital contribution.[11] Thus, the orbital contribution is fixed as −10 K, which gives a set of reasonable parameters: $J_1 = -14.8(3)$ cm^{-1}, $J_2 = 3.6(1)$ cm^{-1}, $g = 2.38(1)$, $\theta = -10$ K, and $R = 1.2 \times 10^{-4}$ (Supporting Information, Figure S7). These results are in agreement with those confirmed in the cobalt hydroxy derivatives:[10] the Co2 atoms sharing two μ_3-OH groups are related by ferromagnetic coupling, whereas antiferromagnetic exchange interactions occur between the Co1 and Co2 atoms. As observed and suggested, ferrimagnetism will occur within such a $\{Co_3(OH)_2\}$ chain.[10,12]

The field-cooled susceptibility in different applied dc fields clearly shows the onset of spontaneous magnetization below 8 K, and the susceptibility increases as the applied field decreases, corresponding to canted antiferromagnetism (Figure 2). Compound **1**·3.7 H_2O exhibits a hysteresis loop at 2 K with a coercive field of 60 Oe and remnant magnetization of 1.16 Nβ (Supporting Information, Figure S9). The saturation magnetization is not reached even at the highest field of 70 kOe (Supporting Information, Figure S10). As

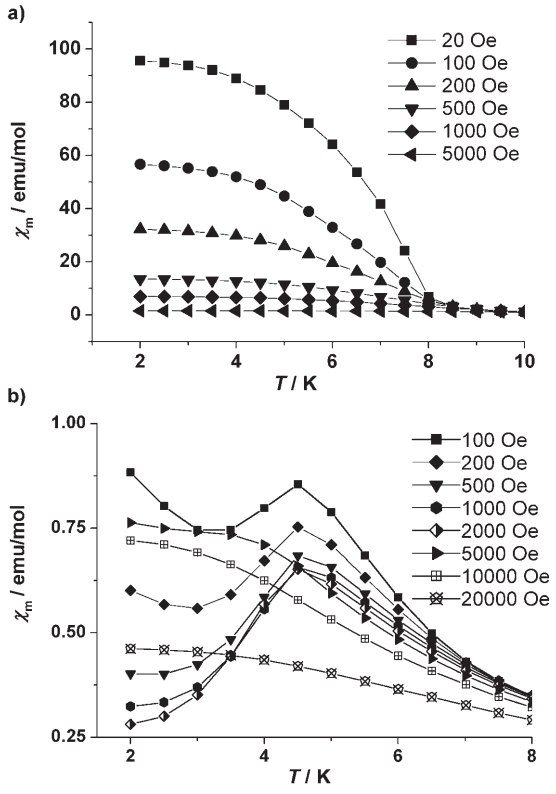

Figure 2. Temperature dependence of the field-cooled magnetic susceptibility of **1**·3.7 H_2O (a) and **1** (b) at various magnetic fields.

shown in Figure 3, both the real χ' and the imaginary χ'' components of the ac susceptibility show a frequency-dependent cusp. This fact indicates a cooperative freezing of the individual magnetic moments, characteristic of spin-

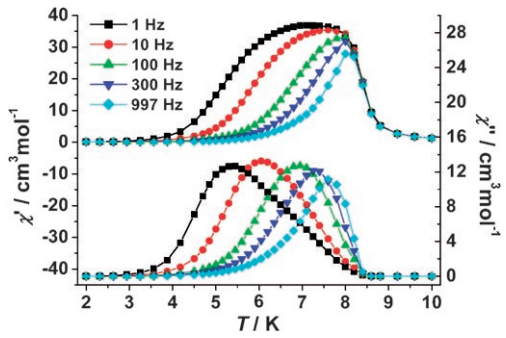

Figure 3. The temperature dependence of the ac magnetic susceptibility of **1**·3.7 H_2O at $H_{ac} = 5$ Oe at various frequencies.

glasses, superparamagnets, or single-chain magnets.[13] The frequency dependence of the ac susceptibility was studied using the equation $\phi = \Delta T_f/[T_f \Delta(\log\omega)]$, where T_f is the freezing temperature and ω is the frequency, and the estimated value of ϕ for **1**·3.7 H_2O is 0.085, which is close to the normal value for superparamagnets and single-chain magnets.[14,15] The fitting of the Arrhenius law, $\tau = \tau_0 \exp(-U/k_BT)$, gives a set of physically reasonable parameters: $\tau_0 = 2.6 \times 10^{-11}$ s and $U/k_B = 122(6)$ K (Supporting Information, Figure S11). The τ_0 value is close to that of 3.0×10^{-11} s observed for the single-chain magnet [Co(hfac)$_2$(NITPhOMe)] (hfac = hexafluoroacetylacetonate, NITPhOMe = 4′-methoxyphenyl-4,4,5,5-tetramethylimidazoline-1-oxyl-3-oxide).[14] At fixed temperatures around the out-of-phase χ'', semicircle Cole–Cole diagrams were obtained (Supporting Information, Figure S12). Thus, the dynamics of the magnetization relaxation in **1**·3.7 H_2O are reminiscent of those of single-chain magnets.[14,15]

To study the solvatomagnetic effect, the magnetic properties of **1** were also investigated. The $\chi_m T$ versus T curve of dehydrated **1** shows a shape similar to that of **1**·3.7 H_2O (Supporting Information, Figure S13). A fitting of the paramagnetic part gives rise to a Curie constant of $C = 8.35$ and a Weiss constant of $\theta = -55.4$ K. The field-cooled susceptibility curves are characteristic of metamagnetism, quite different from those of **1**·3.7 H_2O (Figure 2). The metamagnetism in **1** is in agreement with the sigmoidal curve found for the low-field magnetization (Supporting Information, Figure S14). Although both the real χ' and the imaginary χ'' components are present in the ac susceptibility measurement, the imaginary χ'' component for **1** is much smaller than the real χ' component ($\chi'' \approx 1/250$ of χ'; Supporting Information, Figure S15). Furthermore, the real χ' component is frequency-independent, and the imaginary χ'' component shows very little frequency dependence. The bifurcation for the zero-field and field-cooled magnetic susceptibility curves (Supporting Information, Figure S16) and the presence of a non-zero imaginary χ'' component for **1** indicate a canted antiferromagnetic state at 4.5 K.[1]

The above magnetic behavior can be explained on the basis of ferrimagnetic {$Co_3(OH)_2$} chains. The Co-O-Co angles in both **1**·3.7 H_2O and **1** indicate ferrimagnetic {$Co_3(OH)_2$} chains. At a low field, adjacent chains in **1** are antiferromagnetically coupled through the aromatic btca groups to result in a canted antiferromagnetic state. As the applied field is increased, interchain antiferromagnetic interactions are suppressed to give a ferrimagnetic-like state. Therefore, **1** is characteristic of metamagnetism. For **1**·3.7 H_2O, the interchain weak antiferromagnetic interactions are suppressed by solvent molecules, and thus single-chain-magnet-like behavior was observed as a result of the large interchain distance. Note that a related compound [$Co_3(OH)_2(C_4O_4)_2$]·3 H_2O shows ferromagnetism that arises as a result of smaller Co-O-Co angles and the formation of a brucite-like ribbon.[4e]

In conclusion, the assembly of {$Co_3(OH)_2$} chains and btca resulted in a porous homometallic MOF. The hydrated phase, **1**·3.7 H_2O, shows ferrimagnetism and single-chain-magnet-like behavior while the dehydrated phase, **1**, features field-induced metamagnetism from antiferromagnetism to ferrimagnetism.

Experimental Section

Elemental analyses were performed on a Perkin-Elmer 240 elemental analyzer. The FT-IR spectra were recorded from KBr pellets in range 400–4000 cm^{-1} on a Nicolet 5DX spectrometer. Thermal analysis was carried out in air using SETARAM LABSYS equipment with the heating rate of 10 °C min^{-1}. PXRD data were recorded on a Bruker D8 ADVANCE powder X-ray diffractometer ($Cu_{K\alpha}$, λ = 1.5418 Å). The gas sorption isotherm experiment was performed on a Micromeritics ASAP2010 with nitrogen at 78 K. The magnetic measurements were carried out with Quantum Design SQUID MPMS XL-7 instruments. The diamagnetism of the sample and sample holder were taken into account.

1·3.7 H_2O: A mixture of benzotriazole-5-carboxylic acid (H_2btca; 0.3 mmol, 0.048 g), $Co(NO_3)_2 \cdot 6H_2O$ (0.5 mmol, 0.145 g), CH_3CN (3 mL), and H_2O (2 mL) in a molar ratio of 1:1.7:192:556 was sealed in a 15-mL Teflon-lined stainless container, which was heated to 150 °C and held at that temperature for 5 days. After cooling to room temperature, red crystals of **1**·3.7 H_2O were recovered in 35 % yield by filtration. The bulk phase purity was confirmed by PXRD. Elemental analysis (%) calcd for **1**·3.7 H_2O: C 28.07, H 2.58, N 14.03; found: C 28.01, H 2.56, N 14.05. IR (KBr): $\tilde{\nu}$ = 3425s, 2925w, 2645w, 1635s, 1539m, 1402s, 1265w, 1055m, 788w cm^{-1}.

1: The as-synthesized **1**·3.7 H_2O was heated at 105 °C for 8 h to generate the dehydrated phase **1**. Elemental analysis (%) calcd for **1**: C 31.54, H 1.51, N 15.77; found: C 31.42, H 1.57, N 15.70.

Suitable single crystals of **1**·3.7 H_2O ($0.25 \times 0.08 \times 0.08$ mm^3) and **1** ($0.17 \times 0.08 \times 0.04$ mm^3) were used in the intensity data collection using a Bruker SMART APEX CCD diffractometer at 298(2) K (λ = 0.71073 Å). The structures were solved by direct methods and refined by full-matrix least-squares methods with SHELXTL. All non-hydrogen atoms were refined with anisotropic thermal parameters while the hydrogen atoms of btca ligands were introduced as fixed contributors. The contribution of the solvent to the diffraction pattern in the hydrated phase **1**·3.7 H_2O was subtracted from the observed data by the SQUEEZE method implemented in PLATON. Poor anisotropic thermal parameters and high R-indexes in **1** are due to poor quality of the single crystal resulting from heating and dehydration. Crystal data for **1**·3.7 H_2O: $C_{14}H_8Co_3N_6O_6$: monoclinic, $C2/c$, M_r = 533.05, a = 18.157(11), b = 12.116(7), c = 11.046(7) Å, β = 94.983(10)°, V = 2421(3) $Å^3$, Z = 4, ρ_{calcd} = 1.463 g cm^{-3}, μ =

2.067 mm^{-1}, $T_{min}=0.6261$, $T_{max}=0.8521$, $F(000)=1052$, $R_1=0.0898$ and 0.0505 before and after SQUEEZE, $wR_2=0.3054$ and 0.1212 before and after SQUEEZE, GOF = 0.871. For **1**: $C_{14}H_8Co_3N_6O_6$: monoclinic, $C2/c$, $M_r=533.05$, $a=18.138(5)$, $b=12.127(3)$, $c=11.040(3)$ Å, $\beta=95.189(4)°$, $V=2418.5(11)$ Å^3, $Z=4$, $\rho_{calcd}=1.464$ g cm^{-3}, $\mu=2.069$ mm^{-1}, $T_{min}=0.7199$, $T_{max}=0.9218$, $F(000)=1052$, $R_1=0.1007$, $wR_2=0.2433$, GOF = 1.129. CCDC-623307 and CCDC-624453 contain the supplementary crystallographic data for this paper. These data can be obtained free of charge from The Cambridge Crystallographic Data Centre via www.ccdc.cam.ac.uk/data_request/cif.

Received: October 19, 2006
Revised: December 12, 2006
Published online: March 27, 2007

Keywords: cobalt · magnetic properties · metal–organic frameworks · nanoporous materials

[1] C. J. Kepert, *Chem. Commun.* **2006**, 695 – 700.
[2] G. Férey, *Nat. Mater.* **2003**, *2*, 136 – 137.
[3] a) S. Xiang, X. Wu, J. Zhang, R. Fu, S. Hu, X. Zhang, *J. Am. Chem. Soc.* **2005**, *127*, 16352 – 16353; b) L. G. Beauvais, J. R. Long, *J. Am. Chem. Soc.* **2002**, *124*, 12096 – 12097; c) P. D. C. Dietzel, Y. Morita, R. Blom, H. Fjellvag, *Angew. Chem.* **2005**, *117*, 6512 – 6516; *Angew. Chem. Int. Ed.* **2005**, *44*, 6354 – 6358.
[4] a) G. J. Halder, C. J. Kepert, B. Moubaraki, K. S. Murray, J. D. Cashion, *Science* **2002**, *298*, 1762 – 1765; b) Z. Wang, B. Zhang, H. Fujiwara, H. Kobayashi, M. Kurmoo, *Chem. Commun.* **2004**, 416 – 417; c) A. Rujiwatra, C. J. Kepert, J. B. Claridge, M. J. Rosseinsky, H. Kumagai, M. Kurmoo, *J. Am. Chem. Soc.* **2001**, *123*, 10584 – 10594; d) Y. Sato, S. Ohkoshi, K. Arai, M. Tozawa, K. Hashimoto, *J. Am. Chem. Soc.* **2003**, *125*, 14590; e) M. Kurmoo, H. Kumagai, K. W. Chapman, C. J. Kepert, *Chem. Commun.* **2005**, 3012; f) D. Maspoch, D. Ruiz-Molina, K. Wurst, N. Domingo, M. Cavallini, F. Biscarini, J. Tejada, C. Rovira, J. Veciana, *Nat. Mater.* **2003**, *2*, 190.
[5] N. L. Rosi, J. Kim, M. Eddaoudi, B. Chen, M. O'Keeffe, O. M. Yaghi, *J. Am. Chem. Soc.* **2005**, *127*, 1504 – 1518.
[6] a) S. Nakatsuji, Y. Nambu, H. Tonomura, O. Sakai, S. Jonas, C. Broholm, H. Tsunetsugu, Y. Qiu, Y. Maeno, *Science* **2005**, *309*, 1697 – 1700; b) S. H. Lee, C. Broholm, C. Ratcliff, G. Gasparovic, Q. Huang, T. H. Kim, S. W. Cheong, *Nature* **2002**, *418*, 856 – 858; c) S. T. Bramwell, M. J. P. Gingras, *Science* **2001**, *294*, 1495; d) J. Snyder, J. S. Slusky, R. J. Cava, P. Schiffer, *Nature* **2001**, *413*, 48 – 51.
[7] S. M. Humphrey, P. T. Wood, *J. Am. Chem. Soc.* **2004**, *126*, 13236 – 13237.
[8] A. L. Spek, PLATON, A Multipurpose Crystallographic Tool, Utrecht University, The Netherlands, **1999**.
[9] "Magnetic Behavior of Compounds Containing d^n Ions": A. T. Casey, S. Mitra in *Theory and Applications of Molecular Paramagnetism* (Eds.: E. A. Boudreaux, L. N. Mulay), Wiley, New York, **1976**, pp. 198 – 225.
[10] a) X.-J. Li, X.-Y. Wang, S. Gao, R. Cao, *Inorg. Chem.* **2006**, *45*, 1508 – 1516; b) C. Livage, C. Egger, G. Férey, *Chem. Mater.* **1999**, *11*, 1546 – 1550.
[11] H. Kumagaia, Y. Okab, K. Inouea, M. Kurmoo, *J. Phys. Chem. Solids* **2004**, *65*, 55 – 60.
[12] "One-Dimensional Magnetism: An Overview of the Models": R. Georges, J. J. Borrás-Almenar, E. Coronado, J. Curély, M. Drillon in *Magnetism: Molecules to Materials I*: *Models and Experiments* (Eds.: J. S. Miller, M. Drillon), **2002**, Wiley-VCH, Weinheim, chap. 1, pp. 1 – 47.
[13] J. A. Mydosh, *Spin Glasses*, Taylor and Francis, Washington, DC, **1993**.
[14] A. Caneschi, D. Gatteschi, N. Lalioti, C. Sangregorio, R. Sessoli, G. Venturi, A. Vindigni, A. Rettori, M. G. Pini, M. A. Novak, *Angew. Chem.* **2001**, *113*, 1810 – 1813; *Angew. Chem. Int. Ed.* **2001**, *40*, 1760 – 1763.
[15] a) T.-F. Liu, D. Fu, S. Gao, Y.-Z. Zhang, H.-L. Sun, G. Su, Y.-J. Liu, *J. Am. Chem. Soc.* **2003**, *125*, 13976 – 13977; b) T. Kajiwara, M. Nakano, Y. Kaneko, S. Takaishi, T. Ito, M. Yamashita, A. Igashira-Kamiyama, H. Nojiri, Y. Ono, N. Kojima, *J. Am. Chem. Soc.* **2005**, *127*, 10150 – 10151; c) S. Wang, J.-L. Zuo, S. Gao, Y. Song, H.-C. Zhou, Y.-Z. Zhang, X.-Z. You, *J. Am. Chem. Soc.* **2004**, *126*, 8900 – 8901.

